ZooKeys 1192: 83–102 (2024)
DOI: 10.3897/zookeys.1192.117135

Research Article

A new species of the *Cyrtodactylus chauquangensis* species group (Squamata, Gekkonidae) from Lao Cai Province, Vietnam

Tung Thanh Tran[1], Quyen Hanh Do[2], Cuong The Pham[2,3], Tien Quang Phan[2], Hanh Thi Ngo[4,5,6], Minh Duc Le[4,7,8], Thomas Ziegler[5,6], Truong Quang Nguyen[2,3]

1 *Vinh Phuc College, Phuc Yen City, Vinh Phuc Province, Vietnam*
2 *Institute of Ecology and Biological Resources, Vietnam Academy of Science and Technology, 18 Hoang Quoc Viet Road, Hanoi, Vietnam*
3 *Graduate University of Science and Technology, Vietnam Academy of Science and Technology, 18 Hoang Quoc Viet Road, Cau Giay, Hanoi, Vietnam*
4 *Central Institute for Natural Resources and Environmental Studies, Vietnam National University, 19 Le Thanh Tong, Hanoi, Vietnam*
5 *Cologne Zoo, Riehler Straße 173, 50735, Cologne, Germany*
6 *Institute of Zoology, University of Cologne, Zülpicher Straße 47b, 50674, Cologne, Germany*
7 *Faculty of Environmental Sciences, Hanoi University of Science, Vietnam National University, 334 Nguyen Trai Road, Hanoi, Vietnam*
8 *Department of Herpetology, American Museum of Natural History, Central Park West at 79th Street, New York, New York 10024, USA*
Corresponding author: Truong Quang Nguyen (nqt2@yahoo.com)

OPEN ACCESS

Academic editor: Anthony Herrel
Received: 10 December 2023
Accepted: 1 February 2024
Published: 19 February 2024

ZooBank: https://zoobank.org/9AE17751-35AF-4665-AA7C-C3906D68808F

Citation: Tran TT, Do QH, Pham CT, Phan TQ, Ngo HT, Le MD, Ziegler T, Nguyen TQ (2024) A new species of the *Cyrtodactylus chauquangensis* species group (Squamata, Gekkonidae) from Lao Cai Province, Vietnam. ZooKeys 1192: 83–102. https://doi.org/10.3897/zookeys.1192.117135

Copyright: © Tung Thanh Tran et al. This is an open access article distributed under terms of the Creative Commons Attribution License (Attribution 4.0 International – CC BY 4.0).

Abstract

We describe a new species of the genus *Cyrtodactylus* based on five adult specimens from Bac Ha District, Lao Cai Province, northern Vietnam. *Cyrtodactylus luci* **sp. nov.** is distinguished from the remaining Indochinese bent-toed geckos by a combination of the following morphological characteristics: medium size (SVL up to 89.5 mm); dorsal tubercles in 17–19 irregular transverse rows; ventral scales in 32–34 longitudinal rows at midbody; precloacal pores present in both sexes, 9 or 10 in males, 8 or 9 in females; 12–15 enlarged femoral scales on each thigh; femoral pores 9–12 in males, 5–10 in females; postcloacal tubercles 2–4; lamellae under toe IV 21–23; dorsal pattern consisting of 5 or 6 irregular dark bands, a thin neckband without V-shape or triangle shape in the middle, top of head with dark brown blotches; subcaudal scales transversely enlarged. Molecular phylogenetic analyses recovered the new species as the sister taxon to *C. gulinqingensis* from Yunnan Province, China, with strong support from all analyses and the two taxa are separated by approximately 8.87–9.22% genetic divergence based on a fragment of the mitochondrial ND2 gene. This is the first representative of *Cyrtodactylus* known from Lao Cai Province.

Key words: *Cyrtodactylus luci* sp. nov., gecko, molecular phylogeny, morphology, ND2 gene, taxonomy

Introduction

The *Cyrtodactylus chauquangensis* species group is broadly distributed in the northern Indochina-Burma region, from northern Thailand and Laos to north central and northwestern Vietnam and to southwestern China (Uetz et al. 2023). Taxa within the group are almost exclusively adapted to karst ecosystems. Le et al. (2016) suggested that the group included at least ten species. Grismer et al. (2021a, 2021b) provided a taxonomic review and analyzed phylogenetic relationships of 17 species and one undescribed form from northern Thailand.

The group currently contains 23 recognized species with several taxa recently discovered from Yunnan Province, southern China (Grismer et al. 2021a, 2021b, 2021c; Liu and Rao 2021, 2022).

Lao Cai Province is located in the border area between Vietnam and China with an international borderline of 203 km (Portal of Lao Cai Province 2023). Although Lao Cai contains an area of limestone forest (Portal of Lao Cai Province 2023), no representative of *Cyrtodactylus* has been known from this province so far. On the other hand, members of the genus have been recorded in several neighboring forests, including six species from Yunnan Province of China (*Cyrtodactylus dianxiensis* Liu & Rao, 2021, *C. gulinqingensis* Liu, Li, Hou, Orlov & Ananjeva, 2021, *C. hekouensis* Zhang, Liu, Bernstein, Wang & Yuan, 2021, *C. menglianensis* Liu & Rao, 2022, *C. wayakonei* Nguyen, Kingsada, Rösler, Auer & Ziegler, 2010, *C. zhenkangensis* Liu & Rao, 2021) and five other species reported from Vietnam: one species from Lai Chau (*C. martini* Ngo, 2011) and four species from Son La (*C. bichnganae* Ngo & Grismer, 2010, *C. otai* Nguyen, Le, Pham, Ngo, Hoang, Pham & Ziegler, 2015, *C. sonlaensis* Nguyen, Pham, Ziegler, Ngo & Le, 2017 and *C. taybacensis* Pham, Le, Ngo, Ziegler & Nguyen, 2019).

During our recent field trip in northern Vietnam, we collected five specimens of an unnamed gekkonid species from Bac Ha District, Lao Cai Province, which can be assigned to the *Cyrtodactylus chauquangensis* group based on molecular data. However, the population from Lao Cai Province can be distinguished from congeners by morphological differences and genetic divergence. Therefore, we describe it as a new species in the following.

Materials and methods

Sampling

Field surveys were conducted in Bac Ha District, Lao Cai Province, Vietnam in June 2022 and October 2023 (Fig. 1). After being photographed in life, specimens were anesthetized and euthanized in a closed vessel with a piece of cotton wool containing ethyl acetate (Simmons 2002), fixed in 85% ethanol and subsequently stored in 70% ethanol. Specimens were subsequently deposited in the collections of the Institute of Ecology and Biological Resources (**IEBR**), Hanoi, Vietnam.

Molecular data and phylogenetic analyses

DNA was extracted using DNeasy Blood and Tissue kit (Qiagen, Germany) following manufacturer's instructions. Extracted DNA was amplified by HotStar Taq Mastermix (Qiagen, Germany) with 21 µl volume (10 µl of mastermix, 5 µl of water, 2 µl of each primer at 10 pmol and 2 µl of DNA). PCR conditions were: 95 °C for 15 min to active the taq; with 40 cycles at 95 °C for 30 s, 52 °C for 45 s, 72 °C for 60 s; and the final extension at 72 °C for 6 min. A fragment of the mitochondrial gene, NADH dehydrogenase subunit 2 (ND2), was amplified using the primer pair MetF1 (5'-AAGCTTTCGGGCCCATACC-3') and COIR1 (5'-AGRGTGCCAATGTCTTTGTGRTT-3') (Arevalo et al. 1994; Macey et al. 1997). PCR products were visualized using electrophoresis through a 2% agarose gel stained with ethidium bromide. Successful amplifications were purified to eliminate PCR components using GeneJET™ PCR Purification kit (ThermoFischer

Figure 1. Type locality of *Cyrtodactylus luci* sp. nov. in Lao Cai Province (red circle), Vietnam.

Scientific, Lithuania). Purified PCR products were sent to FirstBase (Malaysia) for sequencing in both directions. We included two samples of the newly discovered population from Lao Cai Province, one of *Cyrtodactylus bichnganae*, one of *C. bobrovi*, one of *C. cucphuongensis*, one of *C. huongsonensis*, one of *C. ngoiensis*, one of *C. sonlaensis*, one of *C. taybacensis*, and one of *C. vilaphongi* along with all available GenBank sequences of these species and other members of the *Cyrtodactylus chauquangensis* group. Two species, *C. hontreensis* and *C. septimontium*, of the *C. intermedius* group, were selected as outgroups (Grismer et al. 2021b). In the end, we were able to incorporate all ingroup taxa (Table 1).

After sequences were aligned by Clustal X v.2.1 (Thompson et al. 1997), data were analyzed using maximum likelihood (ML) as implemented in IQ-TREE (Nguyen et al. 2015), maximum parsimony (MP) implemented in PAUP*4.0b10 (Swofford 2001) and Bayesian inference (BI) as implemented in MrBayes v.3.2.7

Table 1. Species of Cyrtodactylus used in the phylogenetic analysis including localities and GenBank accession numbers of the mitochondrial NADH dehydrogenase subunit 2 (ND2) fragment gene (–: data unavailable).

Species	Locality	Museum number/ Field number	Accession number	Reference
C. auribalteatus	Cambodia: Phnom Aural Wildlife Sanctuary, Kampong Speu Province	–	AP018116	Areesirisuk et al. 2018
Cyrtodactylus luci sp. nov.	Vietnam: Coc Ly Commune, Bac Ha District, Lao Cai Province	IEBR R.5240	PP253960	This study
Cyrtodactylus luci sp. nov.	Vietnam: Coc Ly Commune, Bac Ha District, Lao Cai Province	IEBR R.5241	PP253059	This study
C. bichnganae	Vietnam: Son La City, Son La Province	UNS 0473	MF169953	Brennan et al. 2017
C. bichnganae	Vietnam: Son La City, Son La Province	TBU PAT250	PP253951	This study
C. bobrovi	Vietnam: Ngoc Son – Ngo Luong NR, Lac Son District, Hoa Binh Province	IEBR A.2015.29	MT953471	Grismer et al. 2020
C. bobrovi	Vietnam: Tan Lac, Hoa Binh Province	HB.2015.73	PP253953	This study
C. chauquangensis	Vietnam: Quy Hop District, Nghe An Province	NA 2016.1	MT953475	Grismer et al. 2020
C. cucphuongensis	Vietnam: Cuc Phuong NP, Ninh Binh Province	CP 17.02	MT953477	Grismer et al. 2020
C. cucphuongensis	Vietnam: Cuc Phuong NP, Ninh Binh Province	NHQ.17.71	PP253954	This study
C. doisuthep	Thailand: Doi Phrabart abbey, Chiang Dao District, Chiang Mai Province	AUP–00777	MT497801	Chomdej et al. 2021
C. doisuthep	Thailand: Doi Suthep Mt., Chiang Mai Province	AUP–00774	MT550626	Chomdej et al. 2020
C. dumnuii	Thailand: Chiang Dao, Chiang Mai Province	AUP 00768	MW713972	Grismer et al. 2021
C. erythrops	Thailand: Coral Cave, Pang Mapha District, Mae Hong Son Province	AUP–00771	MT497806	Chomdej et al. 2021
C. erythrops	Thailand: Moe Cham Pae, Mae Hong Son	AUP 00772	MW713958	Grismer et al. 2021b
C. gulinqingensis	China: Gulinqing NR, Maguan County, Wenshan Prefecture, Yunnan Province	KIZ 061813	MZ782150	Liu et al. 2021
C. gulinqingensis	China: Gulinqing NR, Maguan County, Wenshan Prefecture, Yunnan Province	KIZ 061816	MZ782152	Liu et al. 2021
C. gulinqingensis	China: Gulinqing NR, Maguan County, Wenshan Prefecture, Yunnan Province	KIZ 061817	MZ782153	Liu et al. 2021
C. houaphanensis	Laos: near Viengxai, Houaphan Province	IEBR A.2013.109	MW792067	Grismer et al. 2021b
C. huongsonensis	Vietnam: Huong Son, My Duc District, Hanoi City	IEBR A.2011.3A	MT953481	Grismer et al. 2020
C. huongsonensis	Vietnam: Lac Thuy, Hoa Binh Province	HB.2016.44	PP253957	This study
C. hontreensis	Vietnam: Hon Tre Island, Kien Hai District, Kien Giang Province	LSUHC8583	JX440539	Wood et al. 2012
C. martini	Vietnam: Lai Chau Town, Lai Chau Province	UNS 0471	MF169968	Brennan et al. 2017
C. menglianensis	China: Menglian County, Puer City, Yunnan Province	KIZ20210714	OM296043	Liu and Rao 2022
C. menglianensis	China: Menglian County, Puer City, Yunnan Province	KIZ20210716	OM296044	Liu and Rao 2022
C. ngoiensis	Laos: Ngoi District, Luang Prabang Province	IEBR A.20213.100	MW792066	Grismer et al. 2021b
C. ngoiensis	Laos: Ngoi District, Luang Prabang Province	AT2012.1	PP253956	This study
C. otai	Vietnam: Xuan Nha NR, Van Ho District, Son La Province	TBU 2017.2	MT953486	Grismer et al. 2020
C. puhuensis	Vietnam: Pu Hu Nature Reserve, Thanh Hoa Province	ND 01.15	MT953489	Grismer et al. 2020
C. septimontium	Vietnam: Co To Mountain, An Giang Province	NAP 05321	MH940237	Murdoch et al. 2019
C. sonlaensis	Vietnam: Muong Bang Commune, Phu Yen District, Son La Province	IEBR A.2017.1	MT953492	Grismer et al. 2020
C. sonlaensis	Vietnam: Muong Bang Commune, Phu Yen District, Son La Province	IEBR A.2017.2	PP253958	This study
C. soni	Vietnam: Van Long Wetland NR, Gia Vien District, Ninh Binh Province	IEBR R.2016.4	MT953491	Grismer et al. 2020
C. spelaeus	Laos: Kasi District, Vientiane Province	HLM 0315	MW713962	Grismer et al. 2021b
C. taybacensis	Vietnam: Ca Nang Commune, Quynh Nhai District, Son La Province	IEBR 4379	MT953495	Grismer et al. 2020
C. taybacensis	Vietnam: Ta Ma Commune, Tuan Giao District, Dien Bien Province	DB2021.1	PP253952	This study
C. vilaphongi	Laos: Luang Prabang District, Luang Prabang Province	NUOL R–2013.5	PP253955	This study
C. vilaphongi	Laos: Luang Prabang District, Luang Prabang Province	IEBR A.2013.13	MT953497	Grismer et al. 2021b
C. wayakonei	Laos: Ban Nam Eng, Vieng Phoukha District, Luang Nam Tha Province	ZFMK 91016	MT953498	Grismer et al. 2020
C. zhenkangensis	China: Zhenkang County, Lincang City, Yunnan Province	KIZL2020047	MW792062	Grismer et al. 2021b

(Ronquist et al. 2012). For the MP analysis, heuristic analysis was conducted with 100 random taxon addition replicates using tree-bisection and reconnection (TBR) branch-swapping algorithm, with no upper limit set for the maximum number of trees saved. Bootstrap support (BP) was calculated using 1000 pseudo-replicates and 100 random taxon addition replicates. All characters

were equally weighted and unordered. For the ML analysis, we used IQ-TREE v.1.6.8 (Nguyen et al. 2015) with a single model and 10000 ultrafast bootstrap replications (UFB). The optimal model for nucleotide evolution was determined using jModelTest v.1.2.4 (Darriba et al. 2012).

For the BI analysis, we used the optimal model determined by jModelTest with parameters estimated by MrBayes v.3.2.7. Two independent analyses with four Markov chains (one cold and three heated) were run simultaneously for 10^7 generations with a random starting tree and sampled every 1000 generations. Loglikelihood scores of sample points were plotted against generation time to detect stationarity of the Markov chains. Trees generated prior to stationarity were removed from the final analyses using the burn-in function. The posterior probability values (PP) for all nodes in the final majority rule consensus tree were provided. We regard BP ≥ 70% and UFB and PP of ≥ 95% as strong support and values of < 70% and < 95%, respectively, as weak support (Hillis and Bull 1993; Ronquist et al. 2012; Minh et al. 2013).

The optimal model for nucleotide evolution was set to GTR+I+G for ML and BI analysis. The cut-off point for the burn-in function was set to 60, or 0.6% of the total number of trees generated, in the Bayesian analysis, as -lnL scores reached stationarity after 60,000 generations in both runs. Uncorrected pair-wise divergences were calculated in PAUP*4.0b10.

Morphological characters

Measurements were taken with a digital calliper to the nearest 0.1 mm. Abbreviations are as follows: **SVL:** snout-vent length, measured from tip of snout to vent; **TaL:** tail length, measured from vent to tip of tail (* = regenerated); **HL:** head length, measured from tip of snout to retroarticular process of jaw; **HW:** head width, maximum width of head; **HH:** head height, from occiput to underside of jaws; **OrbD:** orbital diameter, greatest diameter of orbit; **SE:** snout to eye distance, from tip of snout to anterior-most point of eye; **EE:** eye to ear distance, from anterior edge of ear opening to posterior corner of eye; **NE:** nares to eye distance, from anterior-most point of eye to posterior-most point of nostril; **ED:** ear length, longest dimension of ear; **ForeaL:** forearm length, from base of palm to tip of elbow; **CrusL:** crus length, from base of heel to knee; **TrunkL:** trunk length, distance from axilla to groin measured from posterior edge of forelimb insertion to anterior edge of hindlimb insertion; **BW:** body width, the widest distance of body; **Internar:** internarial distance, distance between nares; **Interorb:** interorbital distance, shortest distance between left and right supraciliary scale rows.

Scale counts were taken as follows: **SL:** supralabials, counted from the first labial scale to corner of mouth; **IL:** infralabials, counted from the first labial scale to corner of mouth; **N:** nasal scales surrounding nare; **IN:** postrostrals or internasals; **PM:** postmentals; **GST:** granular scales surrounding dorsal tubercles; **V:** ventral scales in longitudinal rows at midbody; **SLB:** number of scales along the midbody from mental to anterior edge of cloaca; **FP:** femoral pores; **PP:** precloacal pores; **PAT:** postcloacal tubercles; **TubR:** tubercle, number of dorsal longitudinal rows of tubercles at midbody between the lateral folds; **EFS:** enlarged femoral scales, number of enlarged femoral scale beneath each thigh; **NSF IV:** number of subdigital lamellae on the fourth finger; **NST IV:** number of subdigital lamellae on the fourth toe. Bilateral scale counts were given as left/right; above sea level (asl).

Multiple Factor Analysis (MFA)

The MFA was also applied in this study using morphometric and meristic characteristics, including SVL, HL, HW, HH, OrbD, SE, EE, ED, ForeaL, CrusL, TrunkL, Internar, Interob and SL, IL, GST, V, TubR, EFS, FP, PP, PAT, NSF IV, NST IV. Other morphological characteristics were not used due to the limitation of available morphometric and meristic data or incomplete sampling (regenerated tail). All statistical analyses were performed using R Core Team (2023). The MFA used six quantitative groups – "SVL", "Head" (including HL, HW, HH), "Eye" (consist of OrbD, SE, EE, ED), "FT" (including ForeaL and CrusL), "TrunkL", "Inter" (consist of Internar and Interorb) and eight qualitative groups – "SpeciesInfor" (including Name of species and ID), "SL-IL" (consist of SL and IL in both sides), "GST_PAT_TubR" (including GST, PAT in both sides and TubR), "V", "EFS" in both sides, "FP" in both sides, "PP", "LIV" (consist of NSF IV and NST IV in left side). To remove the effects of allometry, morphometric data were also normalized to adjust raw data of morphometrics through the allom() function in R package GroupStruct (available at heep://github.com/chankinonn/GroupStruct). Accordingly, the allometric formula is $X_{adj} = \log_{10}(X) - ß[\log_{10}(SVL)-\log_{10}(SVL_{mean})]$, where X_{adj} = adjusted value; X = measured value; ß = unstandardized regression coefficient for each population and SVL_{mean} = overall average SVL of two populations (Thorpe 1975, 1983; Turan 1999; Lleonart et al. 2000; Grismer et al. 2021a; Chan and Grismer 2022). The ordination test was performed using packages Factoextra (Kassambara and Mundt 2017) and FactoMineR (Le et al. 2008) in the software R. The approach was applied to identify active groups and to explain phenotypic variance by estimating the first two Dim values-eigenvalue proportions. Similar coded colors in the MFA scatter plot, surrounded with convex hulls, were presented to visualize the phenotypic spaces of the new species and the most closely related species from China, namely *Cyrtodactylus gulinqingensis* Liu, Li, Hou, Orlov & Ananjeva, 2021; spaces were shown within a spatial coordinate of dimension axes (Dim1 and Dim2). To evaluate the overlap, the loadings of Dim1 and Dim2 of each *Cyrtodactylus* individual were extracted to identify the difference between the two species using the T-test. For all the tests, we applied a significance level of $p < 0.05$.

Results

Phylogenetic analysis

The matrix of molecular data contained 1300 aligned characters, of which 580 were parsimony informative. The MP analysis produced a single most parsimonious tree (tree length = 2359, consistency index = 0.49, retention index = 0.66). Tree topologies from three analyses, ML, MP, and BI were similar and the *Cyrtodactylus* from Bac Ha District, Lao Cai Province was recovered with strong statistical support in all analyses as the sister taxon to *C. gulinqingensis* (BP = 94%; UBP = 100%; PP = 1.00) (Fig. 2). In terms of genetic divergences, the new species is separated from *C. gulinqingensis* by 8.87–9.22% based on a fragment of the mitochondrial ND2 gene. Genetically, it is also significantly divergent from other species within the *C. chauquangensis* group with a pairwise divergence of 12.32–23.85% (Suppl. material 1).

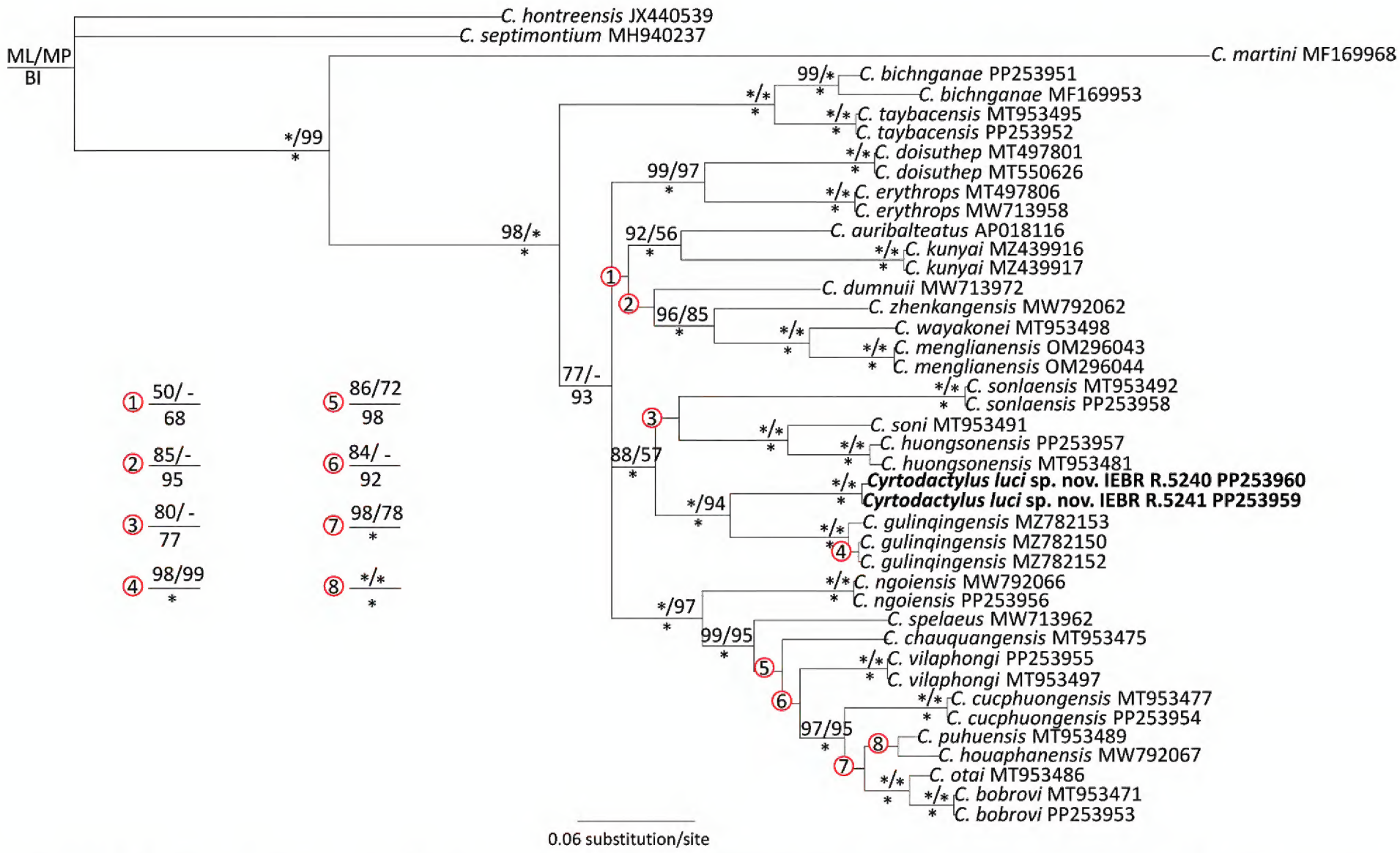

Figure 2. Phylogram based on the Bayesian analysis. Number above and below branches are ML/MP bootstrap and ultrafast bootstrap values and Bayesian posterior probabilities (≥ 50%), respectively. Asterisk and hyphen denote 100% and > 50% values, respectively.

Morphological analysis

Morphologically, the new species from Bac Ha District, Lao Cai Province is closely similar to *C. gulinqingensis* from Yunnan Province, China, however, they plotted separately from each other in MFA (Fig. 3A) and there was a significant difference between two species ($p < 0.05$). The MFA also identified the data set of SVL, Head, Eye, FT, TrunkL, Inter, SL-IL, GST_PAT_TubR, V, EFS, FP, PP as active groups (Fig. 3B). The Eye, FT, Head, Inter, SVL and Trunk groups were the most important in both the first and second multi-factorial dimensions (Fig. 3C, D).

Taxonomy

***Cyrtodactylus luci* sp. nov.**
https://zoobank.org/B03559F4-9C45-4991-8A74-5C346FCD6C37
Figs 4, 5

Type material. *Holotype*. IEBR R.5237 (Field number BH-LC 2022.5), adult male, collected by T.T. Tran, T.Q. Phan and N.H. Nguyen on 30 June 2022, in limestone karst forest near Tham Phuc Village (22°29.514'N, 104°12.416'E, at an elevation of 677 m a.s.l), Coc Ly Commune, Bac Ha District, Lao Cai Province, Vietnam. ***Paratypes*.** IEBR R.5238 (Field number BH-LC 2022.1), IEBR R.5239 (Field number BH-LC 2022.3), adult males and IEBR R.5240, R.5241 (Field numbers BH-LC 2022.2, 2022.4), adult females, bear the same collection data as the holotype.

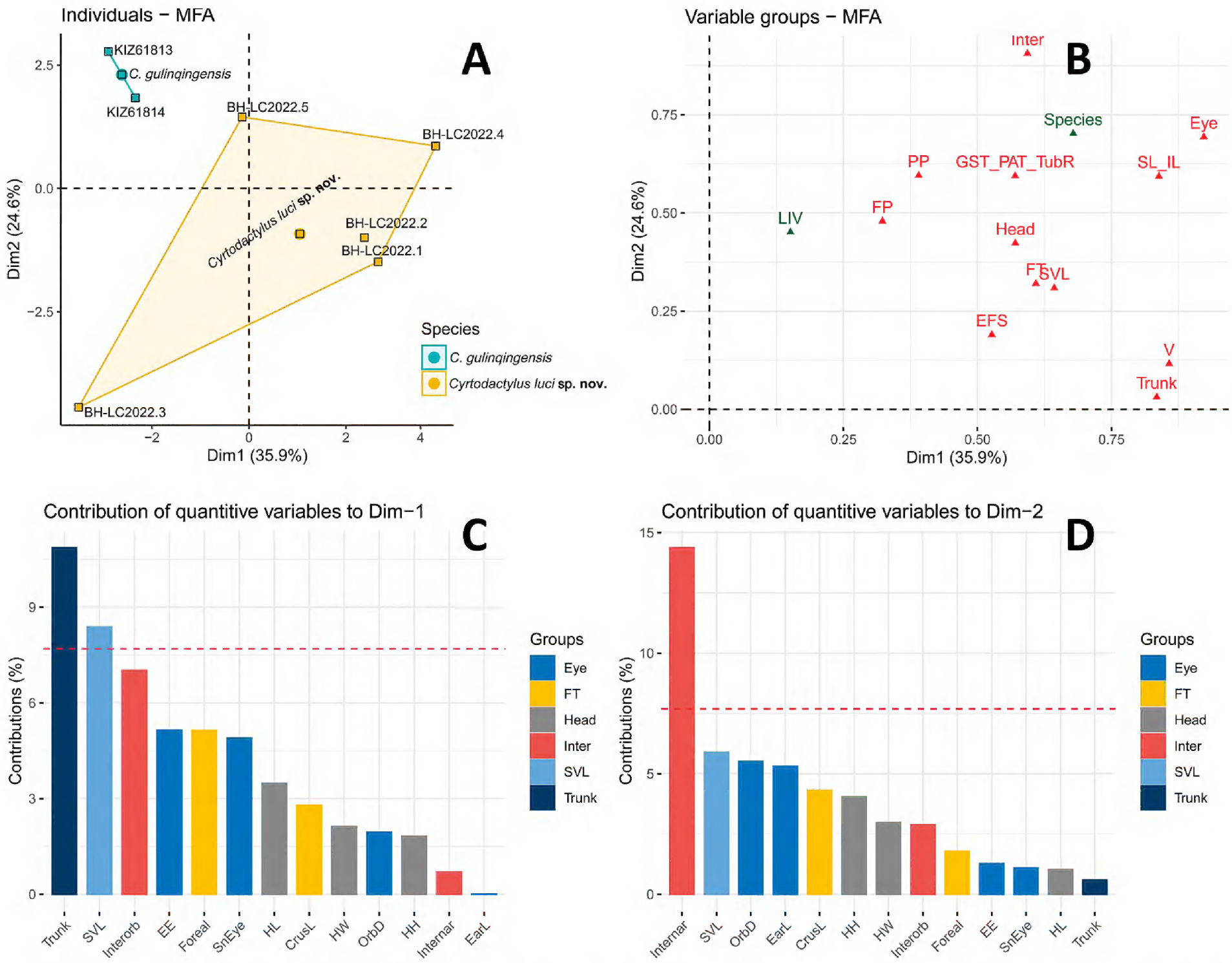

Figure 3. A MFA of *Cyrtodactylus luci* sp. nov. from Vietnam and *C. gulinqingensis* from China **B** scatterplot the groups of all variables for Dim1 and Dim2 axes in the MFA, green triangles as inactive groups of variables, red triangles as active groups of variables **C** bar plot of groups' contribution to the first axes (Dim1) in the MFA **D** bar plot of groups' contribution to the second axes (Dim2) in the MFA.

Diagnosis. The new species can be distinguished from other members of the genus *Cyrtodactylus* by a combination of the following characteristics: Size medium (SVL up to 89.5 mm); dorsal tubercles in 17–19 irregular transverse rows; ventral scales in 32–34 longitudinal rows at midbody; precloacal pores present in both sexual, 9 or 10 in males, 8 or 9 in females; 12–15 enlarged femoral scales on each thigh; femoral pores 9–12 in males, 5–10 in females; postcloacal tubercles 2–4; lamellae under toe IV 21–23; dorsal pattern consisting of 5 or 6 irregular dark bands, a discontinuous thin neckband without V-shape or triangle shape in the middle, dorsal head surface with dark brown blotches; subcaudal scales transversely enlarged.

Description of holotype. Adult male, snout-vent length (SVL) 86.3 mm; body relatively short (TrunkL/SVL 0.4); head distinct from neck, moderately long (HL/SVL 0.28), relatively wide (HW/HL 0.69), slightly depressed (HH/HL 0.41); eye slightly large (OrbD/HL 0.24), pupils vertical; upper eyelid fringe with spinous scales; ear opening below the postocular stripes, obliquely directed and oval, small in size (ED/HL 0.06); two enlarged supranasals, separated from each other anteriorly by one internasal; nares oval, surrounded by supranasal, ros-

tral, first supralabial and three postnasals; loreal region and frontal concave; snout long (SE/HL 0.41), round anteriorly, longer than diameter of orbit (OrbD/SE 0.58); snout scales small, round, granular, larger than those in frontal and parietal regions; rostral wider than high with a medial suture, bordered by first supralabial on each side, nostrils, two supranasals and one internasal; mental triangular, wider than high; postmentals two, enlarged, in contact posteriorly, bordered by mental anteriorly, first infralabial laterally, and an enlarged chin scale posteriorly; supralabials 11/10; infralabials 11/10.

Dorsal scales granular; dorsal tubercles round, keeled, conical, four or five times larger than the size of adjoining scales, each surrounded by 10 granular scales, tubercles forming 17 irregular longitudinal rows at midbody; ventral scales smooth, medial scales 2–3 times larger than dorsal granules, round, subimbricate, largest posteriorly, in 32 longitudinal rows at midbody; lateral folds present, without interspersed tubercles; gular region with homogeneous smooth scales; ventral scales between mental and cloacal slit 170; precloacal groove absent; three rows of enlarged scales present in posterior region of pore-bearing scales; ten precloacal pores arranged in a chevron; 12 or 13 enlarged femoral scales beneath thighs continuous with pore-bearing precloacal scales; femoral pores present on each enlarged femoral scales (except one on right thigh), 24 in total; precloacal pores large, horizontal elongated, positioned in posterior margin of scales; femoral pores small, round, positioned in the center of scales.

Fore and hind limbs moderately slender (ForeaL/SVL 0.16, CrusL/SVL 0.19); dorsal surface of forelimbs covered by few slightly developed tubercles; fingers and toes lacking distinct webbing; subdigital lamellae: finger I 12, finger II 16, finger III 17, finger IV 20, finger V 18, toe I 12, toe II 17, toe III 20, toe IV 21, toe V 20.

Tail regenerated, 104.5 mm in length (generated part 19.5 mm); longer than snout-vent length (TaL/SVL: 1.21); postcloacal tubercles 4/4; subcaudals on original part of tail distinctly transversely enlarged, flat, smooth.

Coloration in life. Ground color of dorsal surface of head, neck, body, limbs and tail light brown. Dorsal surface of head with some dark brown blotches; labial region brown with yellowish cream stripes; skin above the eye gray; eyelid with light yellow color; iris yellow copper with black marking; pupil vertical, elliptical, black; nuchal loop dark brown, discontinous, extending from posterior corner of eye to the neck; tubercles on head, limbs, dorsum light brown to yellow; dorsum with five irregularly-shaped transversal bands and additional irregular smaller blotches; upper surface of limbs with irregular brown marks; six dark brown irregular bands on original part of tail while regenerated part of tail dark gray; chin, throat, chest, belly, lower limbs and ventral surface of tail cream.

Coloration in preservative. The overall color scheme slightly fades in 70% alcohol; yellow color disappeared in preservation while main characteristics are still clearly discernible; dorsal ground color of head, neck, body, limbs and tail grayish brown; color of chin, throat, chest, belly and lower limbs did not change noticeably in preservation.

Sexual dimorphism and variation. The males differ from females in the shape of precloacal pores (larger in males), and the presence of hemipenial swellings at the tail base. For other morphological characteristics see Table 2, Figs 4, 5.

Distribution. *Cyrtodactylus luci* sp. nov. is currently known only from the type locality in Bac Ha District, Lao Cai Province, Vietnam (Fig. 1).

Etymology. The species was named after the zoologist from the Vietnam National Museum of Nature, Vietnam Academy of Science and Technology, late Associate Professor Doctor Luc Van Pham, who contributed greatly to the biodiversity study in Vietnam. For the common names, we suggest Luc's Bent-toed Gecko (English) and Thạch sùng ngón lực (Vietnamese).

Figure 4. Male holotype of *Cyrtodactylus luci* sp. nov. (IEBR R.5237) in life. Photo: T.Q. Phan.

Figure 5. Female paratype of *Cyrtodactylus luci* sp. nov. (IEBR R.5241) in life. Photo: T.Q. Phan.

Natural history. The bent-toed geckos were collected between 19:00 and 22:00, both on limestone cliffs and on trees, about 1.0–1.8 m above the ground. The surrounding habitat was secondary karst forest of medium and small hardwoods mixed with shrubs and vines (Fig. 6). Air temperature was 25.9 °C and relative humidity was 92%.

Comparisons. *Cyrtodactylus luci* sp. nov. is distinguishable from all other members of the *C. chauquangensis* species group by a unique combination of morphological characteristics.

Cyrtodactylus luci sp. nov. differs from *C. auribalteatus* Sumontha, Panitvong & Deein, 2010 by having fewer ventral scale rows (32–34 vs. 38–40 in *C. auribalteatus*), more enlarged femoral scales on each side (12–15 vs. 5–7 in *C. auribalteatus*), more femoral pores on each side in males (9–12 vs. 4 or 5 in *C. auribalteatus*), the presence of femoral pores on each side in females (5–10 vs.

Table 2. Measurements (in mm) and morphological characteristics (abbreviations as in Material and methods) of the type series of *Cyrtodactylus luci* sp. nov. (* = regenerated or broken tail); bilateral meristic characteristics are given as (left/right).

Characters	IEBR R.5237 (Holotype)	IEBR R.5238 (Paratype)	IEBR R.5239 (Paratype)	IEBR R.5240 (Paratype)	IEBR R.5241 (Paratype)	Min–Max
Sex	M	M	M	F	F	
SVL	86.3	88.7	71.7	87.1	89.5	71.7–89.5
TaL	104.5*	107.7	86.2	84.2*	84.1*	86.2–107.7
HL	24.5	24.0	20.3	24.6	25.2	20.3–25.2
HW	16.9	16.6	12.8	17.4	17.4	12.8–17.4
HH	10.1	9.8	7.1	9.7	10.6	7.1–10.6
OrbD	5.9	4.9	4.7	5.1	4.8	4.7–5.9
SE	10.2	10.0	8.4	10.6	10.8	8.4–10.8
EE	6.5	6.6	5.5	6.6	7.2	5.5–7.2
NE	7.5	7.9	6.0	7.7	8.7	6.0–8.7
ED	1.4	1.6	1.9	1.8	1.3	1.4–1.9
ForeaL	14.2	14.2	11.5	14.1	14.4	11.5–14.4
CrusL	16.3	17.2	13.5	16.7	16.8	13.5–17.2
TrunkL	34.4	39.7	31.5	39.7	42.1	31.5–42.1
BW	13.8	14.0	9.4	17.6	19.2	9.4–19.2
Internar	2.8	2.5	2.0	2.7	3.0	2.0–3.0
Interorb	6.9	7.3	5.2	7.6	7.8	5.2–7.8
SL	11/10	11/11	10//10	11/10	11/9	9–11
IL	11/10	12/12	11/13	11/10	9/12	9–13
N	4/4	4/4	4/4	4/4	4/5	4–5
IN	1	1	1	1	1	1
PM	2	3	2	2	2	2
GST	10/10/10	10/10/10	10/9/10	10/10/10	10/10/10	9–10
V	32	34	32	34	34	32–34
SLB	170	171	169	171	166	166–171
FP	12/12	10/9	11/12	10/10	7/5	9–12 in males 5–10 in females
PP	10	9	9	8	9	9–10 in males 8–9 in females
PAT	3/3	4/2	3/3	4/3	3/3	2–4
TubR	17	17	17	19	18	17–19
EFS	13/12	14/15	14/14	13/13	17/15	12–15
NSF IV	18	21	20	19	20	18–21
NST IV	21	23	23	21	23	21–23

absent in *C. auribalteatus*), more precloacal pores in males (9 or 10 vs. 6 in *C. auribalteatus*), the presence of precloacal pores in females (8 or 9 vs. absent in *C. auribalteatus*) and fewer dorsal tubercle rows (17–19 vs. 22–24 in *C. auribalteatus*); from *C. bichnganae* Ngo & Grismer, 2010 by having a smaller size (SVL 71.7–89.5 mm vs. 95.3–99.9 mm in *C. bichnganae*), more ventral scale rows (32–34 vs. 30 or 31 in *C. bichnganae*), more femoral pores on each side in females (5–10 vs. 1 in *C. bichnganae*), and more lamellae under toe IV (21–23 vs. 16–20 in *C. bichnganae*); from *C. bobrovi* Nguyen, Le, Pham, Ngo, Hoang, Pham & Ziegler, 2015 by having fewer ventral scale rows (32–34 vs. 40–45 in *C. bobrovi*), the presence of enlarged femoral scales on each side (12–15 vs. absent in *C. bobrovi*), the presence of femoral pores on each side in males (9–12 vs. absent in *C. bobrovi*) and in females (5–10 vs. absent in *C. bobrovi*), more precloacal pores in males (9 or 10 vs. 5 in *C. bobrovi*), the presence of precloacal pores in females (8 or 9 vs. absent in *C. bobrovi*), and the presence of transversely enlarged subcaudal plates (vs. absent in *C. bobrovi*); from *C. chauquangensis* Hoang, Orlov, Ananjeva, Johns, Hoang & Dau, 2007 by having a smaller size (SVL 71.7–89.5 mm vs. 91.0–99.3 mm in *C. chauquangensis*), fewer ventral scale rows (32–34 vs. 36–38 in *C. chauquangensis*), the presence of enlarged femoral scales on each side (12–15 vs. absent in *C. chauquangensis*), the presence of femoral pores on each side in males (9–12 vs. absent in *C. chauquangensis*) and also in females (5–10 vs. absent in *C. chauquangensis*), more precloacal pores in males (9 or 10 vs. 6 or 7 in *C. chauquangensis*) and also in females (8 or 9 vs. 6 or 7 in *C. chauquangensis*); from *C. cucphuongensis* Ngo & Chan, 2011 by having fewer ventral scale rows (32–34 vs. 42 in *C. cucphuongensis*), the presence of femoral pores on each side in males (9–12 vs. absent in *C. cucphuongensis*) and in females (5–10 vs. absent in *C. cucphuongensis*) and the presence of precloacal pores in males (9–10 vs. absent in *C. cucphuongensis*); from *C. doisuthep* Kunya, Panmongkol, Pauwels, Sumontha, Meewasana, Bunkhwamdi & Dangsri, 2015 by the presence of femoral pores on each side in males (9–12 vs. absent in *C. doisuthep*) and in females (5–10 vs. absent in *C. doisuthep*), more precloacal pores in males (9 or 10 vs. 5 or 6 in *C. doisuthep*) and also in females (8 or 9 vs. absent in *C. doisuthep*); from *C. dumnuii* Bauer, Kunya, Sumontha, Niyomwan, Pauwels, Chanhome & Kunya, 2010 by having fewer ventral scale rows (32–34 vs. 40 in *C. dumnuii*), more femoral pores on each side in males (9–12 vs. 6–7 in *C. dumnuii*) and in females (5–10 vs. absent in *C. dumnuii*), more precloacal pores in males (9 or 10 vs. 5 or 6 in *C. dumnuii*) and also in females (8 or 9 vs. 0–7 in *C. dumnuii*) and more lamellae under toe IV (21–23 vs. 19 in *C. dumnuii*); from *C. erythrops* Bauer, Kunya, Sumontha, Niyomwan, Panitvong, Pauwels, Chanhome & Kunya, 2009 by having more ventral scale rows (32–34 vs. 28 in *C. erythrops*), more lamellae under finger IV (18–21 vs. 16 in *C. erythrops*), more lamellae under toe IV (21–23 vs. 20 in *C. erythrops*) and differences in dorsal color pattern (banded vs. blotched in *C. erythrops*); from *C. gulinqingensis* Liu, Li, Hou, Orlov & Ananjeva, 2021 by having more dorsal tubercle rows (17–19 vs. 14–16 in *C. gulinqingensis*), fewer femoral pores on each side in males (9–12 vs. 13–15 in *C. gulinqingensis*) and in females (5–10 vs. 1–3 in *C. gulinqingensis*) and fewer precloacal pores in females (8 or 9 vs. 7 in *C. gulinqingensis*); from *C. houaphanensis* Schneider, Luu, Sitthivong, Teynié, Le, Nguyen & Ziegler, 2020 by having fewer ventral scale rows (32–34 vs. 35 in *C. houaphanensis*), the presence of enlarged femoral scales on each side (12–15 vs. absent in *C. houaphanensis*), the presence of femoral pores on each

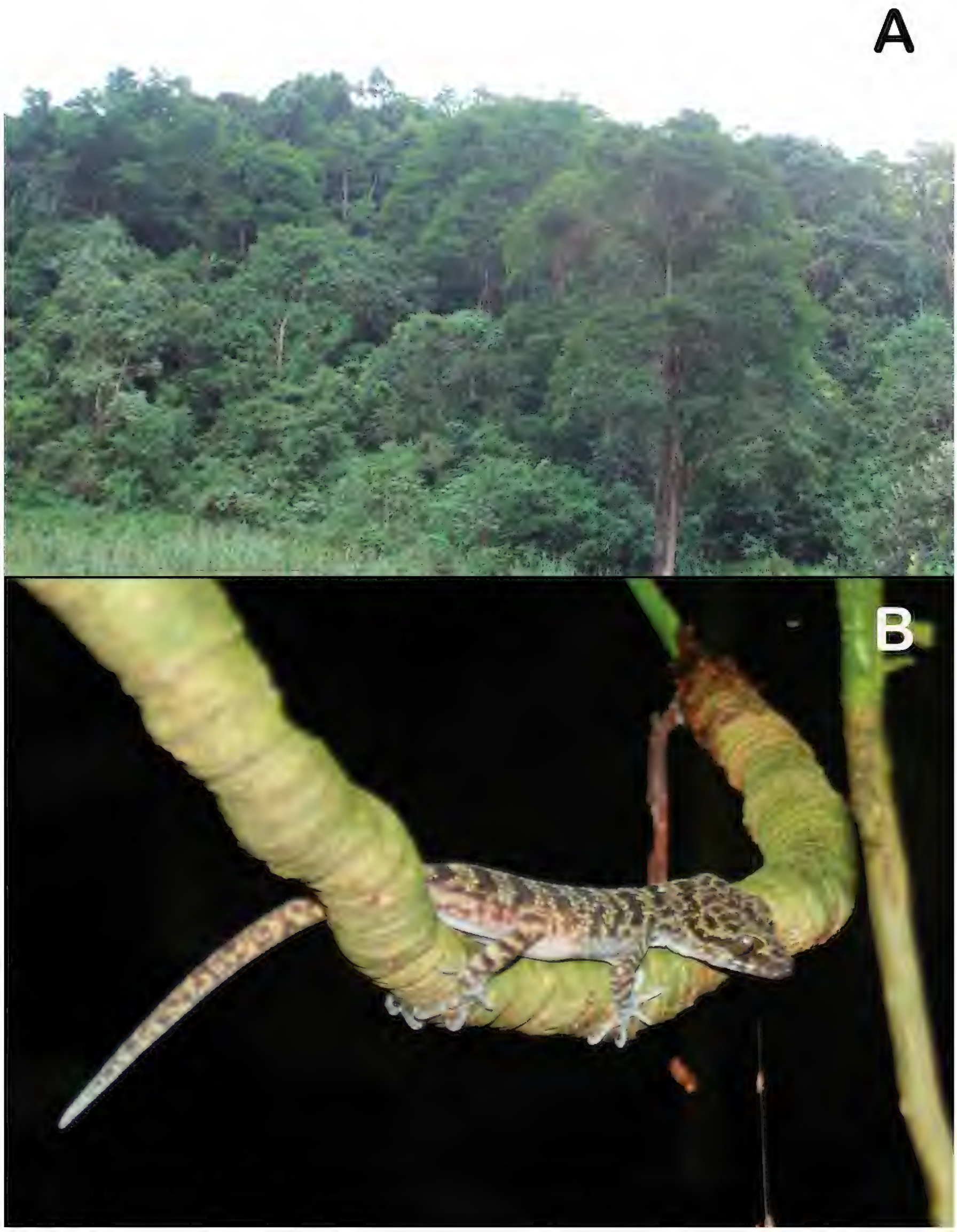

Figure 6. A macrohabitat **B** microhabitat of *Cyrtodactylus luci* sp. nov. Coc Ly Commune, Bac Ha District, Lao Cai Province, Vietnam. Photo: T.Q. Phan.

side in males (9–12 vs. absent in *C. houaphanensis*) and in females (5–10 vs. absent in *C. houaphanensis*) and more precloacal pores in males (9 or 10 vs. 6 in *C. houaphanensis*); from *C. huongsonensis* Luu, Nguyen, Do & Ziegler, 2011 by having fewer ventral scale rows (32–34 vs. 41–48 in *C. huongsonensis*), more

enlarged femoral scales on each side (12–15 vs. 7–9 in *C. huongsonensis*) and more precloacal pores in males (9 or 10 vs. 6 in *C. huongsonensis*); from *C. martini* Ngo, 2011 by having fewer ventral scale rows (32–34 vs. 39–43 in *C. martini*), more precloacal pores in males (9 or 10 vs. 4 in *C. martini*), the presence of precloacal pores in females (8 or 9 vs. absent in *C. martini*) and the presence of transversely enlarged subcaudal plates (vs. absent in *C. martini*); from *C. menglianensis* Liu & Rao, 2022 by having more ventral scale rows (32–34 vs. 26–29 in *C. menglianensis*), the presence of enlarged femoral scales on each side (12–15 vs. absent in *C. menglianensis*), the presence of femoral pores on each side in males (9–12 vs. absent in *C. menglianensis*) and in females (5–10 vs. absent in *C. menglianensis*), more precloacal pores in males (9 or 10 vs. 7 in *C. menglianensis*) and the presence of precloacal pores in females (8 or 9 vs. absent in *C. menglianensis*); from *C. ngoiensis* Schneider, Luu, Sitthivong, Teynié, Le, Nguyen & Ziegler, 2020 by having fewer ventral scale rows (32–34 vs. 38–43 in *C. ngoiensis*), more enlarged femoral scales on each side (12–15 vs. 7–10 in *C. ngoiensis*), more femoral pores on each side in males (9–12 vs. 7 in *C. ngoiensis*) and in females (5–10 vs. absent in *C. ngoiensis*), more precloacal pores in males (9 or 10 vs. 7 in *C. ngoiensis*) and in females (8 or 9 vs. 7 in *C. ngoiensis*) and more lamellae under toe IV (21–23 vs. 19–20 in *C. ngoiensis*); from *C. otai* Nguyen, Le, Pham, Ngo, Hoang, Pham & Ziegler, 2015 by having fewer ventral scale rows (32–34 vs. 38–43 in *C. otai*), the presence of enlarged femoral scales on each side (12–15 vs. absent in *C. otai*), the presence of femoral pores on each side in males (9–12 vs. absent in *C. otai*) and in females (5–10 vs. absent in *C. otai*), more precloacal pores in males (9 or 10 vs. 7 or 8 in *C. otai*), the presence of precloacal pores in females (8 or 9 vs. absent in *C. otai*), and the presence of transversely enlarged subcaudal plates (vs. absent in *C. otai*); from *C. puhuensis* Nguyen, Yang, Le, Nguyen, Orlov, Hoang, Nguyen, Jin, Rao, Hoang, Che, Murphy & Zhang, 2014 by having fewer ventral scale rows (32–34 vs. 36 in *C. puhuensis*), the presence of femoral pores on each side in males (9–12 vs. absent in *C. puhuensis*) and in females (5–10 vs. absent in *C. puhuensis*), and more precloacal pores in males (9 or 10 vs. 5 in *C. puhuensis*); from *C. soni* Le, Nguyen, Le & Ziegler, 2016 by having fewer ventral scale rows (32–34 vs. 41–45 in *C. soni*), more dorsal tubercle rows (17–19 vs. 10–13 in *C. soni*), more enlarged femoral scales on each side (12–15 vs. 8–11 in *C. soni*), more femoral pores on each side in males (9–12 vs. 6–8 in *C. soni*), and more precloacal pores in males (9 or 10 vs. 6 or 7 in *C. soni*); from *C. sonlaensis* Nguyen, Pham, Ziegler, Ngo & Le, 2017 by having more dorsal tubercle rows (17–19 vs. 13–15 in *C. sonlaensis*), fewer femoral pores on each side in males (9–12 vs. 14–15 in *C. sonlaensis*), the presence of femoral pores on each side in females (5–10 vs. absent in *C. sonlaensis*), more precloacal pores in males (9 or 10 vs. 8 in *C. sonlaensis*) and the presence of precloacal pores in females (8 or 9 vs. absent in *C. sonlaensis*); from *C. spelaeus* Nazarov, Poyakov, Orlov, Nguyen, Milto, Martynov, Konstantinov & Chulisov, 2014 by having fewer ventral scale rows (32–34 vs. 36–39 in *C. spelaeus*), the presence of enlarged femoral scales on each side (12–15 vs. absent in *C. spelaeus*), the presence of femoral pores on each side in males (9–12 vs. absent in *C. spelaeus*) and in females (5–10 vs. absent in *C. spelaeus*) and differences in dorsal color pattern (banded vs. blotched in *C. spelaeus*); from *C. taybacensis* Pham, Le, Ngo, Ziegler & Nguyen, 2019 by having more dorsal tubercle rows (17–19 vs. 13–16 in *C. taybacensis*), the presence of femoral pores on each side in males (9–12 vs. absent in *C. taybacensis*)

and in females (5–10 vs. absent in *C. taybacensis*), fewer precloacal pores in males (9 or 10 vs. 11–13 in *C. taybacensis*) and more lamellae under toe IV (21–23 vs. 16–20 in *C. taybacensis*); from *C. vilaphongi* Schneider, Nguyen, Le, Nophaseud, Bonkowski & Ziegler, 2014 by having more dorsal tubercle rows (17–19 vs. 15–16 in *C. vilaphongi*), the presence of enlarged femoral scales on each side (12–15 vs. absent in *C. vilaphongi*), the presence of femoral pores on each side in females (5–10 vs. absent in *C. vilaphongi*) and in females (8 or 9 vs. absent in *C. vilaphongi*), more lamellae under toe IV (21–23 vs. 18–20 in *C. vilaphongi*), and the presence of transversely enlarged subcaudal plates (vs. absent in *C. vilaphongi*); from *C. wayakonei* Nguyen, Kingsada, Rosler, Auer & Ziegler, 2010 by the presence of enlarged femoral scales on each side (12–15 vs. absent in *C. wayakonei*), the presence of femoral pores on each side in males (9–12 vs. absent in *C. wayakonei*) and in females (5–10 vs. absent in *C. wayakonei*), more precloacal pores in males (9 or 10 vs. 6–8 in *C. wayakonei*) and in females (8 or 9 vs. 7 in *C. wayakonei*), and more lamellae under toe IV (21–23 vs. 19–20 in *C. wayakonei*); from *C. zhenkangensis* Liu & Rao, 2021 by having fewer dorsal tubercle rows (17–19 vs. 20–24 in *C. zhenkangensis*), more femoral pores on each side in males (9–12 vs. 2–5 in *C. zhenkangensis*) and in females (5–10 vs. 0–3 in *C. zhenkangensis*) and the presence of dark-colored nuchal loop (vs. absent in *C. zhenkangensis*).

Discussion

The new species from Bac Ha District, Lao Cai Province, is most similar to *Cyrtodactylus gulinqingensis*, a recently described species from Muguan County, Wenshan Prefecture, Yunnan Province of China (Liu et al. 2021). In terms of geographic distribution, the type locality of *C. luci* is approximately 40 km distant from that of its sister species in China. However, they are distinguished from each other by morphological differences as well as a genetic divergence of 8.87–9.22% (ND2 gene).

Our tree topology (Fig. 2) is similar to that reported in Grismer et al. (2021b). However, while *C. auribalteatus* is recovered as a member of the clade including *C. dumnuii*, *C. wayakonei* and other taxa in this study, it is grouped with the lineage consisting of *C. sonlaensis*, *C. huongsonensis* and *C. soni* in Grismer et al. (2021b). According to our phylogenetic analyses, the new species and *C. gulinqingensis* from Yunnan cluster with the latter clade with strong nodal support provided only by BI (Fig. 2). In addition to *C. luci* and *C. gulinqingensis*, the other species in the group occur in Son La (*C. sonlaensis*) and Ninh Binh (*C. soni*) provinces and the suburb of Ha Noi City (*C. huongsonensis*), northwestern Vietnam.

In the *Cyrtodactylus chauquangensis* group, except for *C. doisuthep*, a species known from dry evergreen and deciduous dipterocarp forests in Thailand (Kunya et al. 2014), all 23 remaining species are karst dwellers, comprising three species from Yunnan Province of China, five species from northern Laos, four species from northern Thailand, and 12 species from northern Vietnam (Uetz et al. 2023, this study). In terms of altitudinal distribution range, the members of this species group are found at elevations from 17 m (*C. soni*) to 1660 m (*C. doisuthep*) but most of them occur at elevations between 300 and 800 m a.s.l (Kunya et al. 2015; Le et al. 2016). The new species is the 24th species of the *C. chauquangensis* group, the first species from Lao Cai Province and the eastern side of the Red River in Vietnam, and the 53rd species of *Cyrtodactylus* known from Vietnam (Ngo et al. 2022; Uetz et al. 2023).

Acknowledgements

We are grateful to the directorate of the Forest Protection Department of Lao Cai Province for supporting our field work. We thank N.H. Nguyen (Hanoi) for his assistance in the field and T.A. Tran (Hanoi) for providing the map. For the fruitful collaboration within joint research projects, we cordially thank A.H. Le (IEBR, Hanoi), as well as T. Pagel and C. Landsberg (Cologne Zoo). Many thanks to L.L. Grismer (La Sierra) and V.Q. Luu (Hanoi) for their helpful comments on our manuscript.

Additional information

Conflict of interest

The authors have declared that no competing interests exist.

Ethical statement

No ethical statement was reported.

Funding

This research is funded by the National Foundation for Science and Technology Development (NAFOSTED, Grant No. 106.05-2021.19). Doctoral research of HT Ngo in Germany is funded by the German Academic Exchange Service (DAAD).

Author contributions

Conceptualization: TQN. Data curation: TQP, HTN, QHD, CTP, TTT. Formal analysis: HTN, CTP, MDL, QHD. Funding acquisition: TQN. Investigation: TQP, TTT. Methodology: MDL, TZ, TQN. Supervision: TQN, TZ. Writing - original draft: HTN, TQN, QHD. Writing - review and editing: MDL, HTN, TZ, CTP, TQP, TTT, TQN.

Author ORCIDs

Tung Thanh Tran https://orcid.org/0000-0001-7648-1179
Quyen Hanh Do https://orcid.org/0000-0002-9437-4673
Cuong The Pham https://orcid.org/0000-0001-5158-4526
Tien Quang Phan https://orcid.org/0000-0002-2738-5364
Hanh Thi Ngo https://orcid.org/0000-0002-5283-6243
Minh Duc Le https://orcid.org/0000-0002-2953-2815
Thomas Ziegler https://orcid.org/0000-0002-4797-609X
Truong Quang Nguyen https://orcid.org/0000-0002-6601-0880

Data availability

All of the data that support the findings of this study are available in the main text or Supplementary Information.

References

Areesirisuk P, Muangmai N, Kunya K, Singchat W, Sillapaprayoon S, Lapbenjakul S, Thapana W, Kantachumpoo A, Baicharoen S, Rerkamnuaychoke B, Peyachoknagul S, Han K, Srikulnath K (2018) Characterization of five complete *Cyrtodactylus* mitogenome structures reveals low structural diversity and conservation of repeated sequences in the lineage. PeerJ 6: e6121. https://doi.org/10.7717/peerj.6121

Arevalo E, Davis SK, Sites JW (1994) Mitochondrial DNA sequence divergence and phylogenetic relationships among eight chromosome races of the *Sceloporus grammicus* complex (Phrynosomatidae) in central Mexico. Systematic Biology 43(3): 387–418. https://doi.org/10.1093/sysbio/43.3.387

Bauer AM, Kunya K, Sumontha M, Niyomwan P, Panitvong N, Pauwels OSG, Chanhome L, Kunya T (2009) *Cyrtodactylus erythrops* (Squamata: Gekkonidae), a new cave-dwelling gecko from Mae Hong Son Province, Thailand. Zootaxa 3811(1): 251–261. https://doi.org/10.11646/zootaxa.2124.1.4

Bauer A, Kunya K, Sumontha M, Niyomwan P, Pauwels OSG, Chanhome L, Kunya T (2010) *Cyrtodactylus dumnuii* (Squamata: Gekkonidae), a new cave-dwelling gecko from Chiang Mai Province, Thailand. Zootaxa 2570(1): 41–50. https://doi.org/10.11646/zootaxa.2570.1.2

Brennan IG, Bauer AM, Ngo TV, Wang YY, Wang WZ, Zhang YP, Murphy RW (2017) Barcoding utility in a mega-diverse, cross-continental genus: Keeping pace with *Cyrtodactylus* geckos. Scientific Reports 7(1): e5592. https://doi.org/10.1038/s41598-017-05261-9

Chan KO, Grismer LL (2022) GroupStruct: An R package for allometric size correction. Zootaxa 5124(4): 471–482. https://doi.org/10.11646/zootaxa.5124.4.4

Chomdej S, Pradit W, Suwannapoom C, Pawangkhanant P, Nganvongpanit K, Poyarkov NA, Che J, Gao Y, Gong S (2021) Phylogenetic analyses of distantly related clades of bent-toed geckos (genus *Cyrtodactylus*) reveal an unprecedented amount of cryptic diversity in northern and western Thailand. Scientific Reports 11(1): 2328. https://doi.org/10.1038/s41598-020-70640-8

Darriba D, Taboada GL, Doallo R, Posada D (2012) jmodelTest 2: More models, new heuristicsand high–performance computing. Nature Methods 9(8): e772. https://doi.org/10.1038/nmeth.2109

Grismer LL, Wood Jr PL, Le MD, Grismer JL (2020) Evolution of habitat preference in 243 species of Bent-toed geckos (Genus *Cyrtodactylus* Gray, 1827) with a discussion of karst habitat conservation. Ecology and Evolution 10(24): 13717–13730. https://doi.org/10.1002/ece3.6961

Grismer LL, Suwannapoom C, Pawangkhanant P, Nazarov RA, Yushchenko PV, Naiduangchan M, Le MD, Luu VQ, Poyarkov NA (2021a) A new cryptic arboreal species of the *Cyrtodactylus brevipalmatus* group (Squamata: Gekkonidae) from the uplands of western Thailand. Vertebrate Zoology 71: 723–746. https://doi.org/10.3897/vz.71.e76069

Grismer LL, Wood Jr PL, Poyarkov NA, Le MD, Kraus F, Agarwal I, Oliver PM, Nguyen SN, Nguyen TQ, Karunarathna S, Welton LJ, Stuart BL, Luu VQ, Bauer AM, O'Connell KA, Quah ESH, Chan KO, Ziegler T, Ngo H, Nazarov RA, Aowphol A, Chomdej S, Suwannapoom C, Siler CD, Anuar S, Ngo TV, Grismer JL (2021b) Phylogenetic partitioning of the third-largest vertebrate genus in the world, *Cyrtodactylus* Gray,1827 (Reptilia; Squamata; Gekkonidae) and its relevance to taxonomy and conservation. Vertebrate Zoology 71: 101–154. https://doi.org/10.3897/vertebrate-zoology.71.e59307

Grismer LL, Wood Jr PL, Poyarkov NA, Le MD, Karunarathna S, Chomdej S, Suwannapoom C, Qi S, Liu S, Che J, Quah E, Kraus F, Oliver P, Riyanto A, Pauwels O, Grismer J (2021c) Karstic landscapes are foci of species diversity in the world's third-largest vertebrate genus *Cyrtodactylus* Gray, 1827 (Reptilia: Squamata; Gekkonidae). Diversity 13(5): 1–15. https://doi.org/10.3390/d13050183

Hillis DM, Bull JJ (1993) An empirical test of bootstrapping as a method for assessing confidence in phylogenetic analysis. Systematic Biology 42(2): 182–192. https://doi.org/10.1093/sysbio/42.2.182

Hoang QX, Orlov NL, Ananjeva NB, Johns AG, Hoang TN, Dau VQ (2007) Description of a new species of the genus *Cyrtodactylus* Gray, 1827 (Squamata: Sauria: Gekkonidae) from the karst of North Central Vietnam. Russian Journal of Herpetology 14: 98–106.

Kassambara A, Mundt F (2017) Factoextra: extract and visualize the result of multivariate data analyses. [r package, version 1.0.5.999]

Kunya K, Panmongkol A, Pauwels O, Sumontha M, Meewasana J, Bunkhwamdi W, Dangsri S (2014) A new forest-dwelling Bent-toed Gecko (Squamata: Gekkonidae: *Cyrtodactylus*) from Doi Suthep, Chiang Mai Province, northern Thailand. Zootaxa 3811(2): 251–261. https://doi.org/10.11646/zootaxa.3811.2.6

Kunya K, Sumontha M, Panitvong N, Dongkumfu W, Sirisamphan T, Pauwels O (2015) A new forest-dwelling Bent-toed Gecko (Squamata: Gekkonidae: *Cyrtodactylus*) from Doi Inthanon, Chiang Mai Province, northern Thailand. Zootaxa 3905: 573–584. https://doi.org/10.11646/zootaxa.3905.4.9

Le S, Josse J, Husson F (2008) FactoMiner: A Package for Multivariate Analysis. Journal of Statistical Software 25(1): 1–18. https://doi.org/10.18637/jss.v025.i01

Le DT, Nguyen TQ, Le MD, Ziegler T (2016) A new species of *Cyrtodactylus* (Squamata: Gekkonidae) from Ninh Binh Province, Vietnam. Zootaxa 4162(2): 268–282. https://doi.org/10.11646/zootaxa.4162.2.4

Liu S, Rao DQ (2021) A new species of *Cyrtodactylus* Gray, 1827 (Squamata, Gekkonidae) from Yunnan, China. ZooKeys 1021: 109–126. https://doi.org/10.3897/zookeys.1021.60402

Liu S, Rao D (2022) A new species of *Cyrtodactylus* Gray, 1827 (Squamata, Gekkonidae) from southwestern Yunnan, China. ZooKeys 1084: 83–100. https://doi.org/10.3897/zookeys.1084.72868

Liu S, Li Q, Hou M, Orlov NL, Ananjeva NB (2021) A new species of *Cyrtodactylus* Gray (Squamata, Gekkonidae) from southern Yunnan, China. Russian Journal of Herpetology 28(4): 185–196. https://doi.org/10.30906/1026-2296-2021-28-4-185-196

Lleonart J, Salat J, Torres GJ (2000) Removing allometric effects of body size in morphological analysis. Journal of Theoretical Biology 205(1): 85–93. https://doi.org/10.1006/jtbi.2000.2043

Luu VQ, Nguyen TQ, Do HQ, Ziegler T (2011) A new *Cyrtodactylus* (Squamata: Gekkonidae) from Huong Son limestone forest, Hanoi, northern Vietnam. Zootaxa 3129(1): 39–50. https://doi.org/10.11646/zootaxa.3129.1.3

Macey JR, Larson A, Ananjeva NB, Fang Z, Papenfuss TJ (1997) Two novel gene orders and the role of light-strand replication in rearrangement of the vertebrate mitochondrial genome. Molecular Biology and Evolution 14(1): 91–104. https://doi.org/10.1093/oxfordjournals.molbev.a025706

Minh BQ, Nguyen MAT, von Haeseler A (2013) Ultrafast approximation for phylogenetic bootstrap. Molecular Biology and Evolution 30(5): 1188–1195. https://doi.org/10.1093/molbev/mst024

Murdoch ML, Grismer LL, Wood Jr PL, Thy N, Poyarkov NA, Tri NV, Aowphol A, Pauwels OSB, Grismer JL (2019) Six new species of the *Cyrtodactylus intermedius* complex (Squamata: Gekkonidae) from the Cardamom Mountains and associated highlands of Southeast Asia. Zootaxa 4554(1): 1–62. https://doi.org/10.11646/zootaxa.4554.1.1

Nazarov RA, Poyarkov Jr NA, Orlov NL, Nguyen SN, Milto KD, Martynov AA, Konstantinov EL, Chulisov AS (2014) A review of genus *Cyrtodactylus* (Reptilia: Sauria: Gekkonidae) in fauna of Laos with description of four new species. Trudy Zoologicheskogo Instituta 318(4): 391–423. https://doi.org/10.31610/trudyzin/2014.318.4.391

Ngo TV (2011) *Cyrtodactylus martini*, another new karst-dwelling *Cyrtodactylus* Gray, 1827 (Squamata: Gekkonidae) from Northwestern Vietnam. Zootaxa 2834(1): 33–46. https://doi.org/10.11646/zootaxa.2834.1.3

Ngo TV, Chan KO (2011) A new karstic cave-dwelling *Cyrtodactylus* Gray (Squamata: Gekkonidae) from northern Vietnam. Zootaxa 3125: 51–63.

Ngo TV, Grismer LL (2010) A new karst dwelling *Cyrtodactylus* (Squamata: Gekkonidae) from Son La Province, northwestern Vietnam. Hamadryad 35: 84–95. https://doi.org/10.11646/zootaxa.3835.1.4

Ngo HT, Do QH, Pham CT, Luu VQ, Grismer LL, Ziegler T, Nguyen VTH, Nguyen TQ, Le MD (2022) How many more species are out there? Current taxonomy substantially underestimates the diversity of bent-toed geckos (genus *Cyrtodactylus*) in Laos and Vietnam. ZooKeys 1097: 135–152. https://doi.org/10.3897/zookeys.1097.78127

Nguyen TQ, Kingsada P, Rösler H, Auer M, Ziegler T (2010) A new species of *Cyrtodactylus* (Squamata: Gekkonidae) from northern Laos. Zootaxa 2652(1): 1–16. https://doi.org/10.11646/zootaxa.2652.1.1

Nguyen SN, Yang JX, Le NTT, Nguyen LT, Orlov NL, Hoang CV, Nguyen TQ, Jin J-Q, Rao D-Q, Hoang TN, Che J, Murphy RW, Zhang YP (2014) DNA barcoding of Vietnamese bent-toed geckos (Squamata: Gekkonidae: *Cyrtodactylus*) and the description of a new species. Zootaxa 3784(1): 48–66. https://doi.org/10.11646/zootaxa.3784.1.2

Nguyen TQ, Le MD, Pham AV, Ngo HN, Hoang CV, Pham CT, Ziegler T (2015) Two new species of *Cyrtodactylus* (Squamata: Gekkonidae) from the karst forest of Hoa Binh Province, Vietnam. Zootaxa 3985(3): 375–390. https://doi.org/10.11646/zootaxa.3985.3.3

Nguyen TQ, Pham AV, Ziegler T, Ngo HT, Le MD (2017) A new species of *Cyrtodactylus* (Squamata: Gekkonidae) and the first record of *C. otai* from Son La Province, Vietnam. Zootaxa 4341(1): 25–40. https://doi.org/10.11646/zootaxa.4341.1.2

Pham AV, Le MD, Ngo HT, Ziegler T, Nguyen TQ (2019) A new species of *Cyrtodactylus* (Squamata: Gekkonidae) from northwestern Vietnam. Zootaxa 4544(1): 360–380. https://doi.org/10.11646/zootaxa.4544.3.3

Portal of Lao Cai Province (2023) Portal of Lao Cai Province. https://www.laocai.gov.vn

R Core Team (2023) R: A language and environment for statistical computing. R Foundation for Statistical Computing, Vienna. https://www.R-project.org/

Ronquist F, Teslenko M, van der Mark P, Ayres DL, Darling A, Höhna S, Larget B, Liu L, Suchard MA, Huelsenbeck JP (2012) MrBayes 3.2: Efficient Bayesian phylogenetic inference and model choice across a large model space. Systematic Biology 61(3): 539–542. https://doi.org/10.1093/sysbio/sys029

Schneider N, Nguyen TQ, Le MD, Nophaseud L, Bonkowski M, Ziegler T (2014) A new species of *Cyrtodactylus* (Squamata: Gekkonidae) from the karst forest of northern Laos. Zootaxa 3835(1): 80–96. https://doi.org/10.11646/zootaxa.3835.1.4

Schneider N, Luu VQ, Sitthivong S, Teynie A, Le MD, Nguyen TQ, Ziegler T (2020) Two new species of *Cyrtodactylus* (Squamata: Gekkonidae) from northern Laos, including new finding and expanded diagnosis of *C. bansocensis*. Zootaxa 4822(4): 503–530. https://doi.org/10.11646/zootaxa.4822.4.3

Simmons JE (2002) Herpetological collecting and collections management. Revised edition. Society for the Study of Amphibians and Reptiles, Herpetological Circular 31: 1–153.

Sumontha M, Panitvong N, Deein G (2010) *Cyrtodactylus auribalteatus* (Squamata: Gekkonidae), a new cave-dwelling gecko from Phitsanulok Province, Thailand. Zootaxa 2370(1): 53–64. https://doi.org/10.11646/zootaxa.2370.1.3

Swofford DL (2001) PAUP*. Phylogenetic Analysis Using Parsimony (*and Other Methods). Version 4. Sinauer Associates, Sunderland, Massachusetts. [program]

Thompson JD, Gibson TJ, Plewniak F, Jeanmougin F, Higgins DG (1997) The ClustalX windows interface: Flexible strategies for multiple sequence alignment aided by quality analysis tools. Nucleic Acids Research 25(24): 4876–4882. https://doi.org/10.1093/nar/25.24.4876

Thorpe RS (1975) Quantitative handling of characters useful in snake systematics with particular reference to intraspecific variation in the Ringed Snake *Natrix natrix* (L.). Biological Journal of the Linnean Society, Linnean Society of London 7(1): 27–43. https://doi.org/10.1111/j.1095-8312.1975.tb00732.x

Thorpe RS (1983) A review of the numerical methods for recognizing and analysing racial differentiation. In: Felsenstein J (Ed.) Numerical Taxonomy. NATO ASI Series, Vol. 1. Springer, Berlin, Heidelberg, 404–423. https://doi.org/10.1007/978-3-642-69024-2_43

Turan C (1999) A note on the examination of morphometric differentiation among fish populations: The Truss System. Turkish Journal of Zoology 23: 259–263.

Uetz P, Hallermann J, Hosek J [Eds] (2023) The Reptile Database. http://www.reptile-database.org [Accessed 01 October 2023]

Wood Jr PL, Heinicke MP, Jackman TR, Bauer AM (2012) Phylogeny of bent-toed geckos (*Cyrtodactylus*) reveals a west to east pattern of diversification. Molecular Phylogenetics and Evolution 65(3): 992–1003. https://doi.org/10.1016/j.ympev.2012.08.025

Supplementary material 1

Pair-wise genetic distance between samples used in this study

Authors: Tung Thanh Tran, Quyen Hanh Do, Cuong The Pham, Tien Quang Phan, Hanh Thi Ngo, Minh Duc Le, Thomas Ziegler, Truong Quang Nguyen

Data type: xlsx

Copyright notice: This dataset is made available under the Open Database License (http://opendatacommons.org/licenses/odbl/1.0/). The Open Database License (ODbL) is a license agreement intended to allow users to freely share, modify, and use this Dataset while maintaining this same freedom for others, provided that the original source and author(s) are credited.

Link: https://doi.org/10.3897/zookeys.1192.117135.suppl1